

Theoretical Studies on Quasi-Adiabatic Electronic Effects in Lithium Heavily-Doped Polyacetylene

Hideharu Nobutoki

Advanced Technology R&D Center, Mitsubishi Electric Corporation, 1-1 Tsukaguchi-Honmachi 8-Chome, Amagasaki, Hyogo 661, Japan

Received: December 16, 1996; In Final Form: March 14, 1997[⊗]

A quasi-adiabatic crystal orbital (CO) theory earlier developed has been applied to lithium heavily-doped *trans*-polyacetylene (*t*-PA) to study quasi-adiabatic electronic effects in a metallic state. It has been shown that the quasi-adiabatic electronic structure largely changes from the adiabatic electronic structure. This change arises from the strong interaction of the crystal momentum coupling between carbon π and lithium canonical COs. The coupling also leads to occurrence of a large spin-density-wave (biradical character) in the quasi-adiabatic electronic state. The occurrence has been analyzed to be due to a large electron–electron repulsive interaction. The quasi-adiabatic electronic structure has been discussed with a focus on the electron–electron repulsion.

Introduction

Conjugated conducting polymers have been extensively studied as they are expected to be useful in many applications.^{1,2} Of these polymers, polyacetylene (PA) is well-known to be a basic and famous conjugated organic polymer. A great number of experimental and theoretical investigations on PA have been undertaken.³ Special interest has been paid to this heavily-doped polymer, i.e., when the defects interact strongly, since it will exhibit metallic properties of high conductivity,^{4,5} far-infrared absorption,^{6,7} and high magnetic susceptibility.^{7–11} It has been widely recognized that the appearance of the metallic state in the heavily-doped regime of PA comes from the band closure of the original highest occupied and lowest unoccupied (π – π^*) bands. Occurrence of this closure has been explained in terms of a regular form induced by heavy doping or, in other words, a soliton lattice formation.^{12,13} Alternatively, the occurrence has also been elucidated in terms of a polaronic lattice formation.^{14,15}

To investigate theoretically the lattice deformation as mentioned above, crystal orbital (CO) calculations on heavily-doped PAs have been successfully carried out.^{13,16–21} However, the conventional crystal orbital (CO) calculations only give adiabatic electronic structures. The adiabatic electronic structures here mean that electrons move infinitely slowly on one partially-filled band along the k -space and remain on the same band up to the zone boundary.^{22,23} On the other hand, one should take care, in metallic states, that there will be a finite probability of breakdown of the adiabatic electronic structures when electrons move with a finite velocity.²⁴ In other words, there will be a finite probability that electrons will change from one band to the other vacant band (band crossing), that is, diabatic electronic structures.^{22,23} Such a diabatic electronic structure might influence chemical and physical properties in heavily-doped PAs since the metallic properties measured would be associated with the electrons moving with a finite velocity.

We previously proposed a quasi-diabatic CO theory with the localized crystal orbital transformation to study the electronic structure representing the diabatic behavior of electrons.²³ This method is characterized by a quasi-diabatic treatment of the coupling between canonical COs due to the derivative operator

of crystal momentum. This technique has been successfully applied to nondoped alternating *trans*-PA (*t*-PA) and has proved to be very useful for estimating and analyzing quasi-diabatic electronic structures. In this paper, the method has been applied to the lithium heavily-doped *t*-PA with a regular form (soliton lattice) to study quasi-diabatic electronic effects in a metallic state. The quasi-diabatic electronic structure is also analyzed in terms of occupation numbers and spin-density-waves (SDWs) from a point of electronic correlation.

Method of Calculations

The details of the theoretical treatment have already been described previously.²³ Here, the outline of the method is briefly mentioned. The following procedure has been derived from the electronic Hamiltonian H that is represented as a function of crystal momentum k .

To deal with the diabatic states on the basis of adiabatic (canonical) wave functions, an estimate of k –coupling between these wave functions is required. Thus, the crystal momentum coupling matrix \mathbf{S} has been defined, from the canonical COs $\phi_m(k)$ and $\phi_j(k)$, by a power series expansion in the deviation d from the k -point as follows:

$$S_{mj} = \delta_{mj} + S_{mj}^{(1)}d + O(d^2) \quad (1)$$

where δ_{mj} is the Kronecker delta and

$$S_{mj}^{(1)} = \langle \phi_m(k) | \partial \phi_j(k) / \partial k \rangle \quad (2)$$

Note that the $\phi_j(k)$ can be expanded, in terms of the S_{mj} , by the canonical COs $\{\phi_m(k-d)\}$:

$$\phi_j(k) = \sum_m S_{mj} \phi_m(k-d) \quad (3)$$

The product of the coupling matrix \mathbf{S} and its adjoint \mathbf{S}^\dagger yields the following Hermitian matrix, \mathbf{R} , as a rearrangement matrix to make quasi-diabatic electronic wave functions:

$$\mathbf{R} = \mathbf{S}^\dagger \mathbf{S} \quad (4)$$

The matrix \mathbf{R} can be diagonalized by a unitary transformation \mathbf{T} .

[⊗] Abstract published in *Advance ACS Abstracts*, May 1, 1997.

$$\mathbf{RT} = \mathbf{T}\gamma \quad (5)$$

Then, by the use of eigenvectors \mathbf{T} and eigenvalues γ , transformations of the canonical COs $\phi(k)$ and $\phi(k-d)$ simultaneously may be performed, satisfying the following relation:

$$S'_{mj} = \delta_{mj} \quad (6)$$

where S'_{mj} represents the crystal momentum coupling matrix for the newly transformed orbitals $\phi'_j(k)$ and $\phi'_m(k-d)$. They are given by

$$\phi'_j(k) = \sum_i T_{ij} \phi_i(k) \quad (7)$$

$$\phi'_m(k-d) = \gamma_m^{-1/2} \sum_i \sum_n S_{ni} T_{im} \phi_n(k-d)$$

This transformation is successively performed by varying the k -point in a first Brillouin zone. Equation 6 indicates that the coupling described by the canonical COs is now represented by the transformed COs of eq 7, which are the one-to-one corresponding COs (CCOs) between the $\phi'_j(k)$ and the $\phi'_m(k-d)$.²⁵ The CCOs do not obey the local symmetry of the canonical COs because of the crystal momentum interaction. The CCOs, in other words, the *interactive hybrid* COs, do not have to be either occupied or unoccupied.²⁶ They are something in between, depending on the type of coupling. Accordingly, the change of the occupation number $\nu_i(k)$ of the CCO $\phi'_i(k)$ can be a criterion of the degree of electron transport along k -space in the quasi-diabatic states.^{23,27} Then, the energy dependence of the occupation and the unoccupation (hole) numbers, which we have called "the effective number of free carriers", is given by

$$N_{\text{eff}}(E) = \sum_i \int_{\text{BZ}} \nu_i(k) \delta[E(k) - E_i(k)] dk, \quad \text{for } E \geq E_F \text{ (electrons)} \quad (8)$$

and

$$N_{\text{eff}}(E) = \sum_i \int_{\text{BZ}} [1 - \nu_i(k)] \delta[E(k) - E_i(k)] dk, \quad \text{for } E \leq E_F \text{ (holes)}$$

respectively, where E_F stands for the Fermi energy level. The integration is taken over a first Brillouin zone (BZ).

Results and Discussion

The theory outlined as above was applied to the lithium heavily-doped *t*-PA with a soliton lattice, as shown in Figure 1, where the unit cell is surrounded by broken lines. The carbon backbone of the model doped system used has an equal bond length chain (a soliton lattice) to achieve an idealized metallic state due to the soliton lattice. Geometry of the doped *t*-PA was taken from the calculated result of ref 16. The doped *t*-PA ($\text{C}_3\text{H}_3\text{Li}_1$) corresponds to a doping level of 33%. The calculations have been carried out on the basis of the one-dimensional tight-binding SCF-CO (self-consistent-field-crystal orbital) method at the level of the CNDO/2 (complete neglect of differential overlap, version 2) approximation including all the valence electrons.²⁸ In the calculations of the doped *t*-PA, a screw axis symmetry was employed.

Electronic Structures. First, the conventional band structure and the density of states (DOS) for the Li heavily-doped *t*-PA

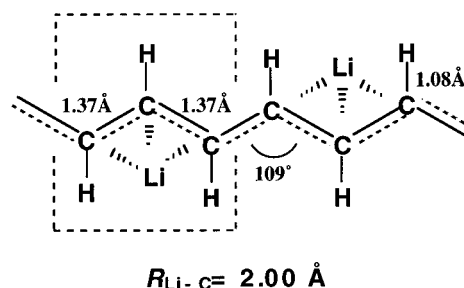


Figure 1. Geometry of the Li heavily-doped *t*-PA used in this study, where $R_{\text{Li-C}}$ stands for lithium-carbon distance.

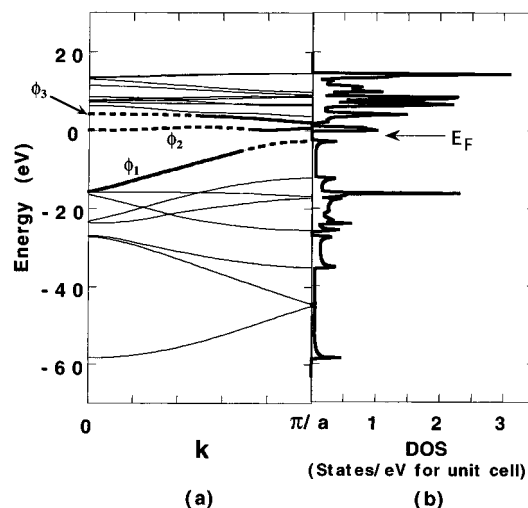


Figure 2. (a) Conventional band structure and (b) the density of states (DOS) for the Li heavily-doped *t*-PA, where the bold line for ϕ_1 , ϕ_2 , and ϕ_3 indicates predominantly carbon π nature and dashed lines predominantly Li nature, around the Fermi energy level (E_F).

are shown in parts a and b of Figure 2, respectively. In Figure 2a, the bold line for ϕ_1 , ϕ_2 , and ϕ_3 indicates predominantly carbon π nature and dashed lines predominantly Li (2s and 2p) nature, around the Fermi energy level (E_F). As is seen, there appears a finite band gap at the E_F due to a charge-density-wave (CDW) instability.¹⁶ Note the charge transfer per Li (carbon) atom of ca. 0.3 (0.1) electron. Next, the CCO band structure and the DOS for the Li heavily-doped *t*-PA, calculated by our method, are shown in parts a and b of Figure 3, respectively. In Figure 3a, the bold for ϕ'_1 , ϕ'_2 , and ϕ'_3 and dashed lines signify predominantly carbon π nature and predominantly Li nature, respectively, around the Fermi energy level (E_F). In contrast to the conventional band structure, the band gap disappears due to a band crossing between ϕ'_1 and ϕ'_2 . They are partially-filled bands at the E_F ; there is a finite CCO-DOS at the E_F . It seems that the structure of the CCO-DOS becomes sharper than that of the conventional DOS, reflecting those differences between the CCO and the conventional band structures.

The optical measurement shows no band gap along with a high magnetic susceptibility on sodium heavily-doped *t*-PA.⁷ In the case of the quasi-diabatic electronic structure based on the soliton lattice, the disappearance of the band gap is associated with the band crossing as mentioned above. The crossing occurs at the point that the canonical COs ϕ_1 and ϕ_2 have both the carbon π and the Li natures most with each other. This suggests that, at that point, the ϕ_1 and the ϕ_2 most strongly interact with each other due to the crystal momentum coupling between them. This is indicative of the hybridization of the carbon π canonical COs onto the Li atom.⁹ Then the CCOs will reflect optical characteristics since the crystal momentum

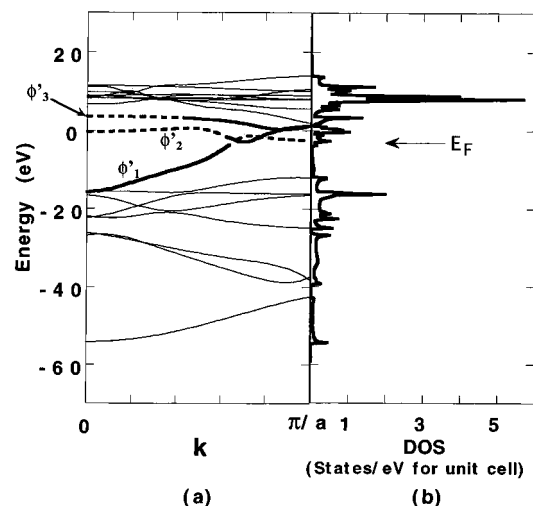


Figure 3. (a) CCO band structure and (b) the DOS for the Li heavily-doped *t*-PA, where bold for ϕ'_1 , ϕ'_2 , and ϕ'_3 and dashed lines signify predominantly carbon π nature and predominantly Li nature, respectively, around the Fermi energy level (E_F).

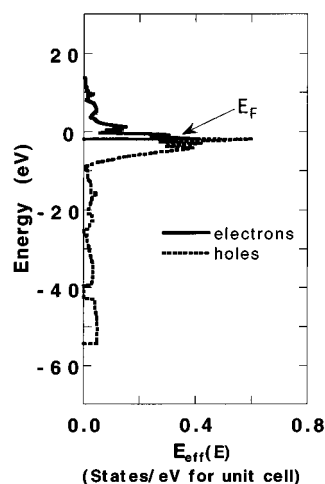


Figure 4. Effective number of free carriers $N_{\text{eff}}(E)$ for the Li heavily-doped *t*-PA, where solid and dotted lines denote the N_{eff} for electrons and for holes, respectively.

coupling operator is directly related to the optical interband transition operator.²⁹ Therefore, the zero band gap optically measured might in part be ascribed to the quasi-diabatic electronic effect based on the crystal momentum coupling.

Alternatively, the zero band gap measured along with the high magnetic susceptibility could be well explained in terms of a half-filled polaron band in a polaron lattice.^{14,15,17} It is remarked that the zero band gap appears due to the partially-filled band at the E_F both on the quasi-diabatic electronic structure in the soliton lattice and on the *adiabatic* polaronic electronic structure in the polaron lattice, although they are different conformations. This implies that the quasi-diabatic electronic state has something to do with the polaronic electronic state, which will be discussed from a point of electronic correlation in the last section.

Effective Number of Free Carriers. Figure 4 illustrates the calculated result of the effective number of free carriers $N_{\text{eff}}(E)$, which is defined by eq 8, to investigate the energy dependence of freely-mobile electrons (holes) for the Li heavily-doped *t*-PA. In this figure, solid and dotted lines denote the N_{eff} values for electrons and for holes, respectively. The N_{eff} shows the existence of the effective “electron” carriers above the E_F and of the effective “hole” carriers below it. It should be given much attention that the N_{eff} has a large value and that

TABLE 1: Effective Number of Free Carriers, N_{eff} , and Ratio (%) of N_{eff} to the Number of Electrons (Holes) N , N_{eff}/N , for the Li Heavily-Doped and the Nondoped *t*-PAs

	$N_{\text{eff}} (N_{\text{eff}}/N)$			
	electrons		holes	
Li-doped	ϕ'_2 ^a	0.33 (17%)	ϕ'_1 ^a	0.58 (29%)
	ϕ'_3 ^a	0.15 (8%)		
nondoped ^b	ϕ'_2 ^c	0.04 (2%)	ϕ'_1 ^c	0.04 (2%)
				0.08 (2%)

^a See figure 3. ^b Previous work taken from ref 23. ^c ϕ'_1 and ϕ'_2 represent the CCOs with π and π^* natures, respectively.

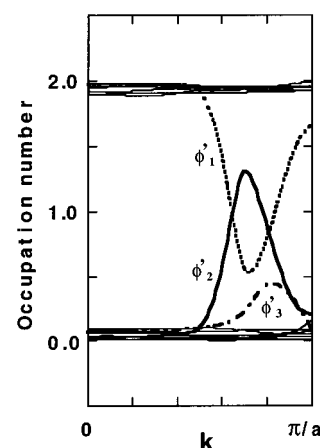


Figure 5. Occupation numbers of the CCOs for the Li heavily-doped *t*-PA.

the N_{eff} value for electrons and for holes is different (electron–hole symmetry broken down) around the E_F . These results are quantitatively summarized concerning the CCOs specified in Table 1, which also lists the corresponding quantities of the nondoped *t*-PA for comparison. Here ϕ'_1 and ϕ'_2 represent the CCOs with π and π^* natures, respectively. The N_{eff} values for the doped *t*-PA are larger than those for the nondoped *t*-PA. This will be partially the evidence for higher intrachain electron (hole) transport in the doped *t*-PA, although electron–phonon and interchain interactions are not taken into account.

In the doped *t*-PA, as is seen, the N_{eff} values mainly arise from the CCOs ϕ'_2 and ϕ'_1 around the E_F . It is important to clarify the consequences of the N_{eff} since energy bands near a E_F determine chemical and physical properties. The N_{eff} values are derived from the occupation number, as described by eq 8. Therefore the behavior of the N_{eff} was analyzed in term of the occupation numbers.

Figure 5 represents the occupation numbers of the CCOs for the Li heavily-doped *t*-PA. It is clearly seen that the occupation numbers of the ϕ'_1 and the ϕ'_2 , indicated by respective dotted and solid lines, largely change, by almost the same amount, around $k = 2\pi/3a$. These orbitals are constructed of carbon π and of Li canonical COs. At the k -point, the canonical COs become a mixed states with carbon π and Li characters most, as previously pointed out. Therefore, the change of the occupation number can be attributed to the strong orbital interaction of the crystal momentum coupling between the mixed states. This is also supported by another change of the occupation number of the ϕ'_3 , as indicated by the broken line, because this orbital is also a mixed state with carbon π and Li characters. From this analysis, it has been found that the large N_{eff} value and this broken electron–hole symmetry arise from the strong crystal momentum interaction between the carbon π

TABLE 2: Ratio of Zwitterionic Configuration to Biradical Configuration r , the Diradical Character y , the Total Spin Angular momentum $\langle S^2 \rangle$, and the Normalized Spin Density $\rho(\text{SD})$ for the Li Heavily-Doped and the Nondoped t -PAs

	k	r	y	$\langle S^2 \rangle$	$\rho(\text{SD})$
Li-doped	0	0.9844	0.0001	0.0309	0.1759
	$2\pi/3a$	0.1414	0.7228	0.9800	0.9899
	π/a	0.9998	0.0000	0.0004	0.0200
nondoped ^a	0	0.9999	0.0000	0.0002	0.0132
	π/a	0.9113	0.0043	0.1695	0.4117

^a Previous work taken from ref 23.

and the Li canonical COs. The Li canonical CO contributes to enhancement of the effective number of free carriers by the interaction.

SDW State. The quasi-diabatic states (CCOs) obtained involve electronic correlation. Our previous study on nondoped t -PA shows that a SDW is produced derived from the electronic correlation in the quasi-diabatic electronic state.²³ Hence, the quasi-diabatic electronic properties in the doped t -PA were analyzed from this respect in the same manner as previously reported.

The singlet wave function of the CCO $\phi'_1(k)$, corresponding to the canonical highest occupied CO $\phi_1(k)$, $^1\Psi(k)$, is given by

$$^1\Psi(k) = N[|\phi'_1 + \overline{\phi'_1}| + |\phi'_1 - \overline{\phi'_1}|] \quad (9)$$

$$= 2^{-1/2} \{C_1[|\chi_a\overline{\chi_b}| + |\chi_b\overline{\chi_a}|] + C_2[|\chi_a\overline{\chi_a}| + |\chi_b\overline{\chi_b}|]\}$$

where C_1 and C_2 are expansion coefficients, N is the normalizing factor, and the bar indicates spin down. The configurations $|\chi_{a(b)}\overline{\chi_{b(a)}}|$ and $|\chi_{a(b)}\overline{\chi_{a(b)}}|$ stand for the biradical (SDW) and the zwitterionic (CDW) singlet pair, respectively, which are defined as follows:

$$\chi_a(k) = 2^{-1/2}(\phi_1(k) + \phi_2(k)) \quad (10)$$

$$\chi_b(k) = 2^{-1/2}(\phi_1(k) - \phi_2(k))$$

The ratio $r = C_2/C_1$ indicates the magnitude of the correlation and has weak ($r = 1.0$) and strong ($r = 0.0$) correlation limits. From the C_1 and C_2 already known, the ratio r , the biradical character y , the total spin angular momentum $\langle S^2 \rangle$, and the normalized spin density $\rho(\text{SD})$ for the CCO $\phi'_1(k)$ were evaluated, as listed in Table 2. Much attention should be given to the case of $k = 2\pi/3a$. As is seen, at this k -point, a SDW largely emerges. In other words, there exists strong electronic correlation. The large SDW comes from a contribution of the canonical CO $\phi_2(k)$ at the point where the strong crystal momentum coupling happens between the π and the Li canonical COs. It is deduced, therefore, that the large SDW arises from this coupling.

An Analysis of the SDW State. The used model of the lithium heavily-doped t -PA itself does not show a SDW on the adiabatic electronic state since the model is given as a neutral state (closed-shell structure) in this study. However, the quasi-diabatic electronic state shows a large SDW. Thus, it is very important and interesting to examine origin of the occurrence of the large SDW in order to manifest the quasi-diabatic electronic effects in the heavily-doped t -PA. For this purpose, an analysis of the SDW state was attempted.

The SDW should be derived from the electron–electron repulsive interaction.³⁰ It should be further remarked that the r value is equivalent to the ratio of the transfer integral (t) and the on-site Coulombic repulsion (U) in the two-center two-electron Hückel–Hubbard model.³¹

$$r = |t|/U \quad (11)$$

Thus, the occurrence of the large SDW ($r = 0.1414$) can be attributed to enlargement of the on-site Coulombic repulsion. This indicates that the electron–electron repulsive interaction becomes large at the k -point so that the electron–electron repulsion turns out to be the large SDW. It has been considered that the enlargement would in part contribute to an increase of conductivity of the doped system since the electron–electron repulsion tends to stiffen the lattice and to oppose dimerization in PA.^{12,32} Note that this means the geometry of carbon–carbon isodistances used in this study remains unchanged due to the quasi-diabatic electronic effect. Moreover, the enlargement of the on-site Coulombic repulsion would help the interchain carrier hopping in the doped systems.³³

The stability of the present SDW state will depend on electron–phonon and interchain interactions that have been ignored. The electron–phonon coupling can drive charge-density-waves (CDWs), leading to a bond-alternating structure (Peierls distortion).³⁰ Hirsch has showed that even for strong electron–phonon coupling a CDW state is enhanced relative to its $U = 0$ value out to $U/t \cong 6$ for the Peierls–Hubbard model, while the CDW state is not enhanced in the strong coupling regime of $U/t > 6$.³⁴ This has been supported within the Hubbard model for fixed values of the electron–phonon coupling in the range relevant to conjugated polymers.³⁵ It is considered, therefore, that the SDW state can still be stable even under electron–phonon interactions since this state ($U/t \cong 7$) lies in the strong coupling regime. On the other hand, interchain interactions can suppress CDWs, through electron–phonon interactions, causing a relaxation of bond alternation.^{36,37} This relaxation has been indeed recognized experimentally.³⁸ Thus the interchain coupling favors the stability of the SDW state. The present SDW state can still be stable under electron–phonon and interchain interactions.

It has been concluded that the quasi-diabatic electronic effects are characterized as the formation of the metallic SDW state. The repulsive interaction plays a dominant role in the quasi-diabatic electronic structure for the heavily-doped t -PA.

Kivelson and Heeger proposed a first-order transition from a soliton lattice to a polaronic lattice which is favored by Coulombic and/or interchain effects.^{14,15} Band calculations, performed by Stafström and Brédas, for different lattice conformations indicated that the presence of the polaronic lattice conformation is in agreement with a large number of experimental (infrared absorption, optical conductivity, magnetic, electron-energy-loss spectroscopy) data.¹⁷ It is noted that the explanation of the appearance of the first-order transition is still an open question.^{12,21} In the first-order transition, Coulombic interactions tend to favor a polaronic lattice: electron–electron repulsion favors the more delocalized charge distribution in a polaron over a soliton.^{14,15} This suggests that the quasi-diabatic electronic state obtained becomes closer to the polaronic state rather than the soliton state. The polaronic state is characterized as a “radical” ion,³⁹ which is due to a half-filled band in the polaronic lattice.^{14,15,18} Appearances of the radical and the half-filled band in the polaronic state are similar to those of the SDW (biradical) and the partially-filled band at the E_F in the quasi-diabatic electronic state, respectively. It has been further considered that the suppression of the dimerization due to the repulsion will lead to the polaron lattice from the soliton lattice.¹⁴ Note that the first-order transition is of a genuine *electronic* phase transition: it occurs without a change in structure.¹² This holds well for the quasi-diabatic electronic structure studied since it is only derived from a genuine electronic transition.

It has been pointed out, therefore, that the quasi-adiabatic electronic state will cause polaronic electronic states; in other words, it may in part assist a transition from a soliton lattice to a polaron lattice.

Conclusions

The proposed quasi-adiabatic CO theory has been applied to the lithium heavily-doped *t*-PA with a soliton lattice to study the quasi-adiabatic electronic effects in a metallic state.

It has been shown that the quasi-adiabatic electronic structure is quite different from the adiabatic electronic structure, for instance, an appearance of a finite CCO-DOS due to the partially-filled bands at the E_F . The effective number of free carriers evaluated for the doped *t*-PA becomes larger than that for the nondoped system. This will be partially the evidence for higher intrachain electron (hole) transport in the doped system due to the quasi-adiabatic electronic effect. It has been found that these phenomena take place induced by the strong interaction of the crystal momentum coupling between the carbon π and the Li canonical COs.

At the E_F , the large SDW appears by the strong crystal momentum coupling. An analysis indicates that the occurrence of the SDW is due to the electron–electron repulsive interaction (enlargement of the on-site Coulombic repulsion). The electron–electron repulsion would increase conductivity of the doped system since the electron–electron repulsion tends to stiffen the lattice and to oppose dimerization in PA. It has been further considered, due to the suppression of the dimerization, that the quasi-adiabatic electronic state will tend to approach the polaronic state rather than the soliton state; the quasi-adiabatic electronic state would cause polaronic electronic states.

It has been concluded that the quasi-adiabatic electronic state is the metallic SDW state for the heavily-doped *t*-PA in which the electron–electron repulsive interaction plays an essential role.

Acknowledgment. I am grateful to Dr. H. Koezuka of my laboratory for useful discussions.

References and Notes

- (1) Skotheim, T. A., Ed. *Handbook of Conducting Polymers*; Marcel Dekker: New York, 1986.
- (2) Brédas, J. L.; Silbey, R., Eds. *Conjugated Polymers: The Novel Science and Technology of Highly Conducting and Nonlinear Optically Active Materials*; Kluwer: Dordrecht, 1991.
- (3) See, for example: Kuzmany, H.; Mehring, M.; Roth, S., Eds. *Electronic Properties of Conjugated Polymers*; Springer Verlag: Berlin, 1987.
- (4) Chiang, C. K.; Fincher, C. R.; Park, Y. W.; Heeger, A. J.; Shirakawa, H.; Louis, E. J.; Gau, S. C.; MacDiarmid, A. G. *Phys. Rev. Lett.* **1977**, *39*, 1098.
- (5) Moses, D.; Denenstien, A.; Chen, J.; Heeger, A. J.; McAndrew, P.; Woerner, T.; MacDiarmid, A. G. *Phys. Rev.* **1982**, *B25*, 7652.
- (6) Tanner, B. D.; Doll, G. L.; Rao, A. M.; Eklund, P. C.; Arbuckle, G. A.; MacDiarmid, A. G. *Synth. Met.* **1989**, *28*, D141.
- (7) Chung, T.-C.; Feldblum, A.; Heeger, A. J.; MacDiarmid, A. G. *J. Chem. Phys.* **1981**, *74*, 5504.
- (8) Chen, J.; Chung, T.-C.; Moraes, F.; Heeger, A. J. *Solid State Commun.* **1985**, *53*, 757.
- (9) Moraes, F. J.; Chen, J.; Chung, T.-C.; Heeger, A. J. *Synth. Met.* **1985**, *11*, 271.
- (10) Winokur, W.; Moon, Y. B.; Heeger, A. J.; Barker, J.; Bott, D. C.; Shirakawa, H. *Phys. Rev. Lett.* **1987**, *58*, 2329.
- (11) Yang, X. Q.; Tanner, B. D. *Solid State Commun.* **1987**, *61*, 335.
- (12) Heeger, A. J.; Kivelson, S.; Schrieffer, J. R.; Su, W.-P. *Rev. Mod. Phys.* **1988**, *60*, 781.
- (13) Tanaka, K.; Yamabe, T. *Adv. Quantum Chem.* **1985**, *17*, 251.
- (14) Kivelson, S.; Heeger, A. J. *Phys. Rev. Lett.* **1985**, *55*, 308.
- (15) Kivelson, S.; Heeger, A. J. *Synth. Met.* **1987**, *17*, 183.
- (16) Brédas, J. L.; Chance, R. R.; Silbey, R. J. *Phys. Chem.* **1981**, *85*, 756.
- (17) Stafström, S.; Brédas, J. L. *Phys. Rev.* **1988**, *B38*, 4180.
- (18) Kertész, M.; Vonderviszt, F.; Pekker, S. *Chem. Phys. Lett.* **1982**, *90*, 430.
- (19) Kertész, M. *Int. J. Quantum Chem.* **1986**, *29*, 1165.
- (20) Tanaka, K.; Mayumi, O.; Koike, T.; Yamabe, T. *Synth. Met.* **1989**, *31*, 181.
- (21) Tanaka, K.; Mayumi, O.; Yamabe, T. *Synth. Met.* **1990**, *38*, 395.
- (22) Durand, P.; Malrieu, J.-P. *Adv. Chem. Phys.* **1987**, *67*, 335.
- (23) Nobutoki, H.; Tsunoda, S. *J. Phys. Chem.* **1996**, *100*, 6189.
- (24) See, for example: Ashcroft, N. W.; Mermin, N. D. *Solid State Physics*; Saunders College: Philadelphia, 1976; Chapter 12.
- (25) Amos, A. T.; Hall, G. G. *Proc. R. Soc. London, A* **1961**, *263*, 483.
- (26) Fujimoto, H.; Koga, N.; Fukui, K. *J. Am. Chem. Soc.* **1981**, *103*, 7452.
- (27) Nobutoki, H.; Koezuka, H. *J. Mol. Struct. (THEOCHEM)* **1994**, *310*, 29.
- (28) Imamura, A.; Fujita, H. *J. Chem. Phys.* **1974**, *61*, 115.
- (29) Agrawal, G. P.; Flytzanis, C. *Chem. Phys. Lett.* **1976**, *44*, 366.
- (30) Kiess, H. G., Ed. *Conjugated Conducting Polymers*; Springer Verlag: Berlin, 1974.
- (31) Yamaguchi, K.; Yoshioka, Y.; Takatsuka, T.; Fueno, T. *Theor. Chim. Acta* **1978**, *48*, 185.
- (32) Kivelson, S.; Su, W.-P.; Schrieffer, J. R.; Heeger, A. J. *Phys. Rev. Lett.* **1987**, *58*, 1899.
- (33) Tanaka, K.; Ito, A.; Okada, M.; Yamabe, T. *Synth. Met.* **1992**, *46*, 341.
- (34) Hirsch, J. E., *Low-Dimensional Conductors and Superconductors*; Jérôme, D.; Caron, L. G., Eds.; NATO ASI Series B; Plenum: New York, 1987; Vol. 155, pp 71–86.
- (35) Campbell, D. K.; DeGrand, T. A.; Mazumdar, S. *J. Stat. Phys.* **1986**, *43*, 803.
- (36) Whangbo, M.-H. *Crystal Chemistry and Properties of Materials with Quasi-One-Dimensional Structures*; Rouxel, J., Ed.; Reidel: Dordrecht, 1986; p 27.
- (37) Yoshizawa, K.; Hoffmann, R. *J. Chem. Phys.* **1995**, *103*, 2126.
- (38) See, for example: Roth, S.; Bleier, H. *Adv. Phys.* **1987**, *36*, 385.
- (39) Boudreaux, D. S.; Chance, R. R.; Brédas, J. L.; Silbey, R. *Phys. Rev.* **1983**, *B28*, 6927.